

Photoisomerization and Thermal Isomerization of Arylazoimidazoles

Joe Otsuki,^{*,†} Kazuya Suwa,[†] Kamal Krishna Sarker,[‡] and Chittaranjan Sinha^{*,‡}*College of Science and Technology, Nihon University, 1-8-14 Kanda Surugadai, Chiyoda-ku, Tokyo 101-8308, Japan, and Department of Chemistry, Jadavpur University, Kolkata 700032, India**Received: October 17, 2006; In Final Form: January 3, 2007*

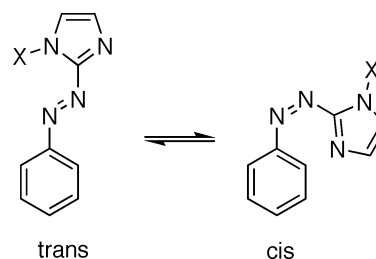
Photoisomerization and thermal isomerization behaviors of an extensive series of arylazoimidazoles are investigated. Absorption spectra are characterized by a structured $\pi\pi^*$ absorption band around 330–400 nm with a tail on the lower energy side extending to 500 nm corresponding to an $n\pi^*$ transition. The trans-to-cis photoisomerization occurs on excitation into these absorption bands. The quantum yields are dependent on the excitation wavelength, as observed for azobenzene derivatives, but are generally larger than those of azobenzene. The thermal cis-to-trans isomerization rates are also generally larger than that of azobenzene and are comparable to those of 4-*N,N*-dimethylaminoazobenzene and 4-nitroazobenzene. Arylazoimidazoles with no substituent on the imidazole nitrogen are unique in that the quantum yield for the trans-to-cis photoisomerization and the rate of thermal cis-to-trans isomerization are particularly large. It is proposed that the fast thermal isomerization is due to an involvement of self-catalyzed and protic molecule-assisted tautomerization to a hydrazone form.

Introduction

Aromatic azo compounds are known for their ability to undergo light-induced and/or thermal cis/trans isomerization. Azobenzene and its derivatives constitute the major class of compounds that have attracted unabated research interest, from viewpoints of basic science and potential applications to molecular switches.^{1–4} Most of the derivatives have substituents on the parent azobenzene scaffold, whereas less attention has been paid to its analogues having a heterocyclic ring in place of the phenyl group. Arylazoimidazoles, among them, constitute an interesting class of heterocyclic azo compounds as a potential switching group in biological applications and in coordination chemistry, because imidazole is a ubiquitous and essential group in biology, especially as a metal coordination site. This family of compounds have been extensively used as ligands for metal ions by CS.^{5–9} and others.^{10–12} However, very few reports concerning the photochromic reactions, as shown in Scheme 1, of arylazoimidazole dyes can be found in the literature. Majima and co-workers prepared (deoxy)ribofuranosyl derivatives of phenylazoimidazole and observed that these compounds undertake reversible cis/trans isomerization.¹³ Very recently, Fukuda and co-workers prepared polymers containing arylazoimidazole dyes that exhibit photoinduced birefringence, although they did not directly observe the photochromic reactions.¹⁴

We have reported the photoisomerization and thermal isomerization behaviors of 2-(phenylazo)imidazole (Pai-H) and its methylated derivative, 1-*N*-methyl-2-(phenylazo)imidazole (Pai-Me).¹⁵ In these studies, we have found that Pai-Me undergoes reversible cis/trans photoisomerization with quantum yields higher than those for azobenzene. The quantum yield of photoisomerization exhibits a wavelength dependence just as for azobenzene derivatives. The thermal cis-to-trans isomerization rate for Pai-H is much larger than that of Pai-Me. It is still

SCHEME 1: Isomerization of Phenylazoimidazole



an open question whether these behaviors are specific to Pai-Me and Pai-H or general for arylazoimidazoles with and without a substituent on the imidazole nitrogen. Herein, we report photoisomerization and thermal isomerization behaviors of an extensive series of arylazoimidazoles, which are shown in Chart 1, to shed light on general substituent and structural effects on the isomerization phenomena.

Experimental Methods

Compounds. Known compounds among those listed in Chart 1 were prepared according to reported procedures.^{16–22} The following novel compounds were prepared in analogous methods.

Cai-MeBn. Anal. Found: C, 65.68; H, 4.89; N, 18.04. Calcd for C₁₇H₁₅ClN₄: C, 65.70; H, 4.87; N, 18.03.

4-Me-Pai-Me. Anal. Found: C, 65.31; H, 5.99; N, 27.72. Calcd for C₁₇H₁₅ClN₄: C, 65.98; H, 6.04; N, 27.98.

4-Me-Pai-Et. Anal. Found: C, 67.26; H, 6.60; N, 26.18. Calcd for C₁₇H₁₅ClN₄: C, 67.27; H, 6.59; N, 26.15.

4-Me-Pai-Bn. Anal. Found: C, 73.90; H, 5.85; N, 20.29. Calcd for C₁₇H₁₅ClN₄: C, 73.89; H, 5.84; N, 20.27.

2-Me-Pai-Et. Gummy. ¹H NMR (CDCl₃): δ 1.52 (3H, t, *J* = 8.0 Hz), 2.37 (3H, s), 4.38 (2H, quartet, *J* = 8.0 Hz), 7.37 (1H, s), 7.53 (3H, m), 7.84 (2H, d, *J* = 8.0 Hz).

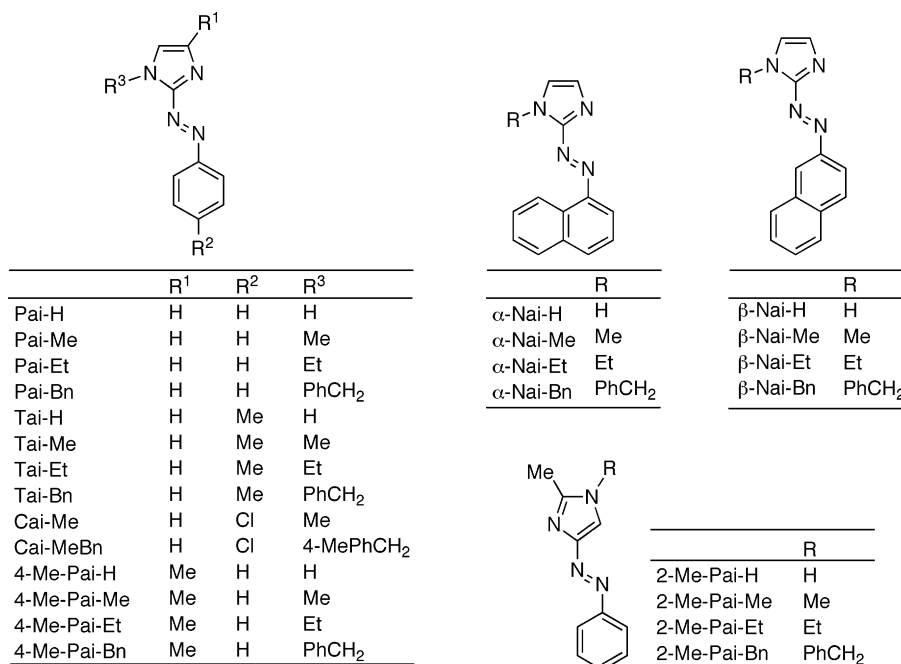
2-Me-Pai-Bn. Gummy. ¹H NMR (CDCl₃): δ 2.38 (3H, s), 5.13 (2H, s), 7.25–7.35 (5H), 7.40 (1H, s), 7.59 (3H, m), 7.80 (2H, d, *J* = 8.0 Hz).

* Corresponding authors. E-mail: otsuki@chem.cst.nihon-u.ac.jp (J.O.); c_r_sinha@yahoo.com (C.S.).

[†] Nihon University.

[‡] Jadavpur University.

CHART 1



Methods. Spectroscopic grade solvents were purchased from Kanto Chemical (methanol, hexane, and acetonitrile) and Wako Pure Chemical Industries (toluene). Absorption spectra were taken with a Shimadzu UV-2400PC spectrometer or a Shimadzu Multispec-1500 photodiode array spectrometer in a 1 × 1 cm quartz optical cell maintained at 25 °C with a Peltier thermostat. The light source of a Shimadzu RF-5300PC fluorimeter was used as an excitation light for photoisomerization reactions. The full width at half-maximum was 4.5 nm. The wavelength values for excitation into the $\pi\pi^*$ and $n\pi^*$ bands were 355 and 454 nm, respectively, for all compounds except for α -Nai-X (X = H, Me, Et, Bn), for which 380 and 500 nm were used. An optical filter was used to cut off overtones when necessary. The absorption spectra of pure cis-isomers were obtained by measuring the absorption spectrum and the ¹H NMR for the same cis-rich mixture of representative compounds (see Supporting Information). Quantum yields (Φ) were obtained by measuring initial trans-to-cis isomerization rates (ν) in a well-stirred solution within the above instrument using the equation

$$\nu = (\Phi I_0/V)(1 - 10^{-\text{Abs}})$$

where I_0 is the photon flux at the front of the cell, V is the volume of the solution, and Abs is the initial absorbance at the irradiation wavelength. The value of I_0 was obtained by using azobenzene ($\Phi_{\pi\pi^*,t\rightarrow c} = 0.11$ and $\Phi_{n\pi^*,t\rightarrow c} = 0.24$)²³ under the same irradiation conditions, except for α -Nai-X, for which Pai-Me ($\Phi_{\pi\pi^*,t\rightarrow c} = 0.25$ and $\Phi_{n\pi^*,t\rightarrow c} = 0.35$)¹⁵ was used. The estimated errors in the values of Φ are $\pm 10\%$. The thermal cis-to-trans isomerization rates were obtained by monitoring absorption changes intermittently for a cis-rich solution kept in the dark at a constant temperature of 25 °C. The estimated errors in the values of $k_{c\rightarrow t}$ are $\pm 3\%$.

Density functional theory (DFT) calculations were carried out using a Gaussian 03w program package²⁴ on a personal computer. We used the B3LYP functional²⁵ and cc-pVDZ basis sets.²⁶

Results and Discussion

Absorption Spectra. Absorption spectra for the arylazoimidazole derivatives displayed in Chart 1 were measured in

methanol, toluene, and hexane. The results obtained in toluene are summarized in Table 1.

The absorption spectrum of Pai-Me in toluene shown in Figure 1a illustrates the characteristics common to phenylazoimidazole derivatives: (1) a structured absorption band around 360 nm with a molar absorption coefficient on the order of $10^4 \text{ M}^{-1} \text{ cm}^{-1}$ and (2) a tail extending into 500 nm. From the analogy with the absorption spectra of azobenzene derivatives, it is likely that the large absorption band around 360 nm corresponds to $\pi\pi^*$ transitions, and the tail corresponds to an $n\pi^*$ transition. The assignment is also supported by theoretical calculations, as described later. The $\pi\pi^*$ absorption peaks (λ_{max}) for derivatives of (2-phenylazo)imidazole are in the range 361–375 nm, which is between the $\pi\pi^*$ absorption bands of azobenzene (313 nm) and 4-*N,N*-dimethylaminoazobenzene (390 nm).²⁷

Replacing the phenyl group by an α -naphthyl group results in bathochromic shifts of the λ_{max} to around 400 nm, whereas the replacement by a β -naphthyl group results in bathochromic shifts to ca. 380 nm (Figure 1b,c). 4-(Phenylazo)imidazoles exhibit absorption spectra similar to those of 2-(phenylazo)imidazoles (Figure 1d). These spectra show little solvent dependence; the $\pi\pi^*$ peak wavelengths differ only by 8 nm at most among the spectra in methanol, toluene, and hexane for most of the compounds investigated. In general, a slight blue shift is recognized on going from nonpolar toluene to polar methanol, suggesting that the ground state is more stabilized than the excited state in a polar solvent.

DFT calculations were carried out to fully understand and identify the absorption spectra and the nature of optical transitions. We used B3LYP²⁵ and cc-pVDZ²⁶ as a functional and a basis set, respectively. First, the geometry was optimized using the standard procedure on the Gaussian program.²⁴ The resulting stable conformations are all nearly planar. There are several nearly equivalent stable conformations for each compound related by a 180° flip about the N(azo)–C(ring) bonds. Then, the frontier orbitals were inspected for the most stable conformation among them. Figure 2 is a pictorial summary of the calculations, and the optimized coordinates are given in the Supporting Information.

TABLE 1: Absorption Spectra and Isomerization of Arylazoimidazoles^a

compounds	trans, $\pi\pi^*$		cis, $\pi\pi^*$		cis, $n\pi^*$		$\phi_{\pi\pi^*,t\rightarrow c}$ ^b	$\phi_{n\pi^*,t\rightarrow c}$ ^c	$k_{c\rightarrow t}/10^{-5} \text{ s}^{-1}$
	$\lambda_{\text{max}}/\text{nm}$	$\epsilon/\text{M}^{-1} \text{ cm}^{-1}$	$\lambda_{\text{max}}/\text{nm}$	$\epsilon/\text{M}^{-1} \text{ cm}^{-1}$	$\lambda_{\text{max}}/\text{nm}$	$\epsilon/\text{M}^{-1} \text{ cm}^{-1}$			
Pai-H ^d	362	18000	306	7000	445	1660	0.23	<i>e</i>	1000 ^f
Pai-Me ^d	363	17000	329	8460	454	1600	0.25	0.35	3.2
Pai-Et	364	12800	321	7260	446	2030	0.26	0.35	4.5
Pai-Bn	365	9860	318	6630	449	1397	0.34	0.43	3.4
Tai-H	364	9430	311	3850	~450 ^f	1010	0.42	<i>e</i>	4300 ^f
Tai-Me	365	17500	320	8200	460	1920	0.18	0.35	4.7
Tai-Et	374	11400	342	5980	449	2190	0.17	0.38	9.9
Tai-Bn	372	15400	316	7670	450	2230	0.16	0.43	9.1
Cai-Me	369	21500	333	9980	454	1950	0.20	0.46	2.7
Cai-MeBn	370	23100	333	10900	457	2320	0.19	0.41	7.9
4-Me-Pai-H	371	19200	297	8190	392	9240	0.18	<i>e</i>	1700 ^f
4-Me-Pai-Me	361	11030	298	5680	443	1930	0.20	0.32	23
4-Me-Pai-Et	375	15900	343	8680	448	3170	0.20	0.43	8.8
4-Me-Pai-Bn	373	10700	333	5330	451	1480	0.28	0.41	7.8
α -Nai-H	395	7000	321	5300	~450 ^g	1300	0.66	<i>e</i>	3600 ^f
α -Nai-Me	396	12070	326	8660	~450 ^g	1900	0.29	0.39	350
α -Nai-Et	397	14500	328	11490	~450 ^g	2200	0.28	0.34	97
α -Nai-Bn	398	11700	328	8140	~450 ^g	1700	0.24	0.34	103
β -Nai-H	376	19800	314	9020	~430 ^g	2500	0.21	0.43	1620 ^f
β -Nai-Me	377	20500	322	12400	452	2460	0.23	0.41	9.7
β -Nai-Et	377	19540	330	10090	463	2430	0.19	0.42	7.6
β -Nai-Bn	378	18300	329	9060	464	2480	0.26	0.43	22
2-Me-Pai-H	355	14000	<i>e</i>	<i>e</i>	<i>e</i>	<i>e</i>	<i>e</i>	<i>e</i>	<i>e</i>
2-Me-Pai-Me	340	13620	298	7380	421	1420	0.30	0.42	0.41
2-Me-Pai-Et	352	7080	<300 ^h	<i>h</i>	420	1830	0.31	0.40	49
2-Me-Pai-Bn	351	10900	313	5420	445	1620	0.35	0.43	12

^a In toluene at 25 °C. ^b Excitation at 355 nm except for α -Nai-X (X = H, Me, Et, Bn) for which 380 nm light was used. ^c Excitation at 454 nm except for α -Nai-X (X = H, Me, Et, Bn) for which 500 nm light was used. ^d Reference 15. ^e Little change upon irradiation. ^f Apparent first-order rate constant under arylazoimidazole concentration of 17 μM . See the main text for details. ^g Broad plateau-like band. ^h Out of the measured range (<300 nm).

The highest-occupied molecular orbitals (HOMOs) are π orbitals delocalized over the whole molecule, in which the N=N double bond is in a bonding interaction. On the other hand, the lowest unoccupied molecular orbitals (LUMOs) are π^* orbitals, extending over the whole molecule as well, which have a node between the azo nitrogen atoms. The *n* orbital on the azo group appears as HOMO-1.

Time-dependent DFT (TD-DFT) calculations were carried out on the optimized structures. The obtained energies and oscillator strengths of transitions are drawn with vertical bars in Figure 1. The comparison of the calculated results with the experimental spectra indicates that the TD-DFT correctly reproduces absorption spectra qualitatively for this class of compounds. The asterisks on the wavelength scale indicate the positions of $n\pi^*$ transitions (HOMO-1 \rightarrow LUMO). The calculations suggest that an $n\pi^*$ transition lies in the low-energy tail of absorption spectrum for each compound, although the calculations give a nil value for the oscillator strength, because of its forbidden nature of the transition. The calculated $\pi\pi^*$ absorption (HOMO \rightarrow LUMO) of Pai-Me appears at 354 nm, which is within 10 nm from the observed λ_{max} (363 nm). For α -Nai-Me, the calculated absorption at 417 nm correctly reproduces the bathochromic shift as compared to that for Pai-Me. This transition corresponds to the $\pi\pi^*$ (HOMO \rightarrow LUMO) transition. The calculations indicate that there are additional transitions at 336 and 330 nm. These are also $\pi\pi^*$ transitions but with a significant charge-transfer component from a naphthalene π to a delocalized π^* (LUMO) orbital. Compared to α -Nai-Me, β -Nai-Me (Et) exhibits a hypsochromically shifted spectrum, which is again reproduced by the calculations. The calculated two transitions at 383 and 347 nm for β -Nai-Me have a significant contribution from the $n\pi^*$ (HOMO-1 \rightarrow LUMO) transition mixed into $\pi\pi^*$ transitions. This is unique for β -Nai-Me among the four compounds investigated. The calculational

results for 2-Me-Pai-Me is almost identical to those for Pai-Me, indicating that the position of substitution on the imidazole ring by the arylazo group has little influence on the property of optical transitions.

Photoisomerization. Upon irradiation of light at the λ_{max} of the $\pi\pi^*$ absorption to a solution of arylazoimidazole, the absorption spectrum changes in a way similar to that observed for the trans-to-cis isomerization of azobenzene derivatives. The intense $\pi\pi^*$ peak decreases, which is accompanied by a slight increase at the tail portion of the spectrum around 450 nm ($n\pi^*$) until a photostationary state is reached. Subsequent irradiation at the newly appeared longer wavelength peak ($n\pi^*$) reverses the course of the reaction and the original spectrum is recovered up to a point, which is another photostationary state under $n\pi^*$ irradiation. Figure 1 includes these spectra at the photostationary states.

The quantum yields of the trans-to-cis photoisomerization were determined using those of azobenzene or Pai-Me as standards, and the results are tabulated in Table 1. A prominent feature of the photoisomerization of azobenzene derivatives is its wavelength-dependent quantum yield. The reported quantum yields are $\Phi_{t\rightarrow c} = 0.11$ and $\Phi'_{t\rightarrow c} = 0.24$ for $\pi\pi^*$ and $n\pi^*$ excitation, respectively, for the pristine azobenzene.²³ The wavelength dependency has also been found in the photoisomerization of Pai-Me in a previous report.¹⁵ Here the dependency has been found to be general. In all cases studied, except those we could not determine the values due to little spectral change upon $n\pi^*$ irradiation, the quantum yields with the longer wavelength irradiation are substantially higher than those with the shorter wavelength excitation.

Another noticeable point is that the photoisomerization quantum yields for arylazoimidazoles are generally larger than those of azobenzene. Thus, we have demonstrated that arylazoimidazole derivatives are quite efficient photochromic com-

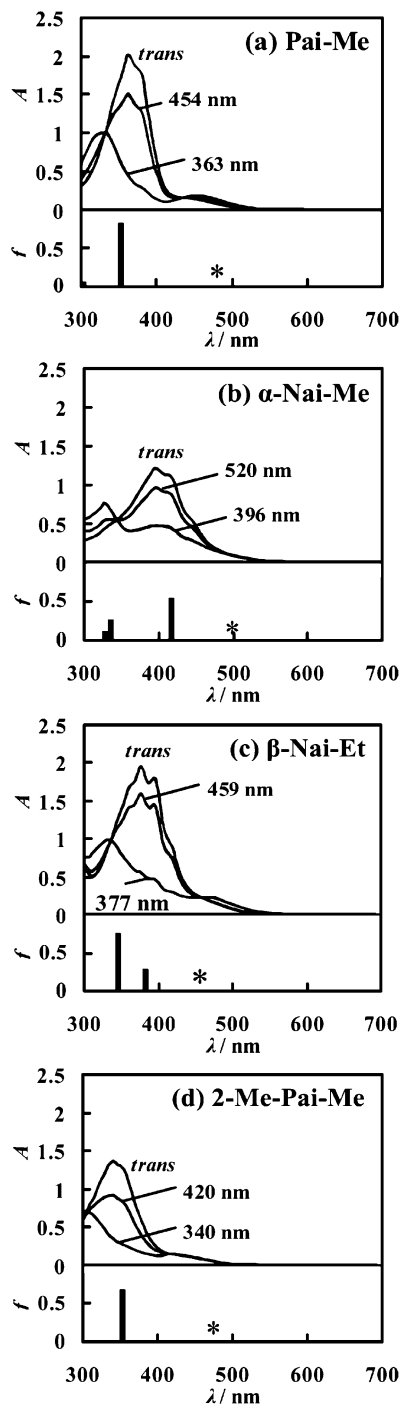


Figure 1. Representative absorption spectra for arylazoimidazoles in toluene (0.1 mM). Spectra of the *trans* isomers and photostationary states under irradiation at the indicated wavelength are given. (a) Pai-Me. (b) α -Nai-Me. (c) β -Nai-Et. (d) 2-Me-Pai-Me. Oscillator strengths obtained from TD-DFT calculations are also given. In (c), the calculation was done for β -Nai-Me instead of β -Nai-Et.

pounds. In particular, the isomerization quantum yields on $\pi\pi^*$ excitation for Tai-H (0.42) and α -Nai-H (0.66) are prominently higher than others.

Thermal Cis-to-Trans Isomerization—General Trends. Thermal cis-to-trans isomerization rates of arylazoimidazoles measured in toluene at 25 °C are collected in Table 1. The rates for most compounds are distributed in a relatively narrow range on the order of 10^{-5} s^{-1} . These are larger than the value reported for azobenzene and rather closer to those of 4-*N,N*-dimethylaminoazobenzene and 4-nitroazobenzene.²⁷ There are some that fall out of this range, however. In particular, arylazoimidazoles

that bear no substituent on the imidazole nitrogen undergo exceptionally fast thermal cis-to-trans isomerization. There seems to be no exception to this tendency. The rates exceeds 10^{-2} s^{-1} for Pai-H, Tai-H, 4-Me-Pai-H, α -Nai-H, and β -Nai-H. The poor conversion to the cis isomer in the case of 2-Me-Pai-H also suggests fast thermal cis-to-trans isomerization. The large rates of thermal cis-to-trans isomerization for arylazoimidazoles without a substituent on the imidazole nitrogen are discussed in the next section in detail.

The group of α -naphthylazoimidazole derivatives also undergo much faster thermal cis-to-trans isomerization than other compounds in the present study, if not as fast as the above-mentioned arylazoimidazoles without a substituent on the imidazole nitrogen. Thus, the rates for α -Nai-Me and α -Nai-Et are on the order of 10^{-3} s^{-1} , more than 1 order of magnitude larger than other phenylazoimidazoles, such as Pai-Me. It has been observed that replacing phenyl group in azobenzene by an α -naphthyl group results in a large increase in the thermal cis-to-trans isomerization rate. The activation energy for the isomerization decreases from 94 kJ mol^{-1} for azobenzene (in heptane)²⁸ to 82 kJ mol^{-1} for α -naphthylazobenzene (in benzene).²⁹

Thermal Cis-to-Trans Isomerization—Non-*N*-Substituted Arylazoimidazoles. As briefly described above with the data collected in Table 1, we can conclude that the fast thermal isomerization is not specific to Pai-H¹⁵ but general for arylazoimidazoles with no substituent on the imidazole nitrogen. Without exception, all compounds with imidazole-NH exhibit much larger thermal isomerization rates than those with a substituent on the imidazole nitrogen, whether it is a 2-(phenylazo) (Pai-H, Tai-H, 4-Me-Pai-H) or naphthylazo (α -Nai-H) derivatives. It is likely that this is also the case for 4-(phenylazo)-derivatives (2-Me-Pai-H). Thus, the presence of the hydrogen on the imidazole nitrogen must be involved in the rapid thermal cis-to-trans isomerization.

Arylazoimidazole without any substituent on the imidazole nitrogen can in principle exist as a hydrazone-type tautomer. However, the X-ray crystal structures^{30,31} and UV-visible spectroscopic studies in solution^{32,33} show that the actual structure is the azo form both in the solid state and in solution. This is consistent with DFT calculations (B3LYP/cc-pVDZ) on Pai-H, which show that the energy of the hydrazone form in the optimized structure, which is of a *trans* and planar structure, is above that of the *trans*-azo form by 18.2 kJ mol^{-1} , as shown in Figure 3. Still, a state above the most stable state only by 18.2 kJ mol^{-1} may be accessible at room temperature in solution. A transition state has been found along the pathway of the hydrogen (Mulliken charge: 0.184) shift reaction connecting the *trans*-azo form and the hydrazone form above the former by 91.2 kJ mol^{-1} .

A metastable planar conformation is found for the *cis*-hydrazone form, the energy of which is above the *cis*-azo form only by 3.3 kJ mol^{-1} . Once the *cis*-azo form has changed into the *cis*-hydrazone form, the cis-to-trans isomerization should be facile, because the relevant N–N bond is now formally a single bond.^{34,35} Another stationary state of the hydrazone form is found wherein the imidazole and phenyl planes are mutually nearly perpendicular. The structure of this state, which lies above the *cis*-hydrazone form by merely 9.0 kJ mol^{-1} , may be close to the transition state of the cis-to-trans isomerization of the hydrazone form. The experimental activation energy for the cis-to-trans isomerization in the azo form was found to be 79 kJ mol^{-1} for Pai-Me,¹⁵ which is also shown in Figure 3 for comparison. If there is a reaction pathway through a hydrazone

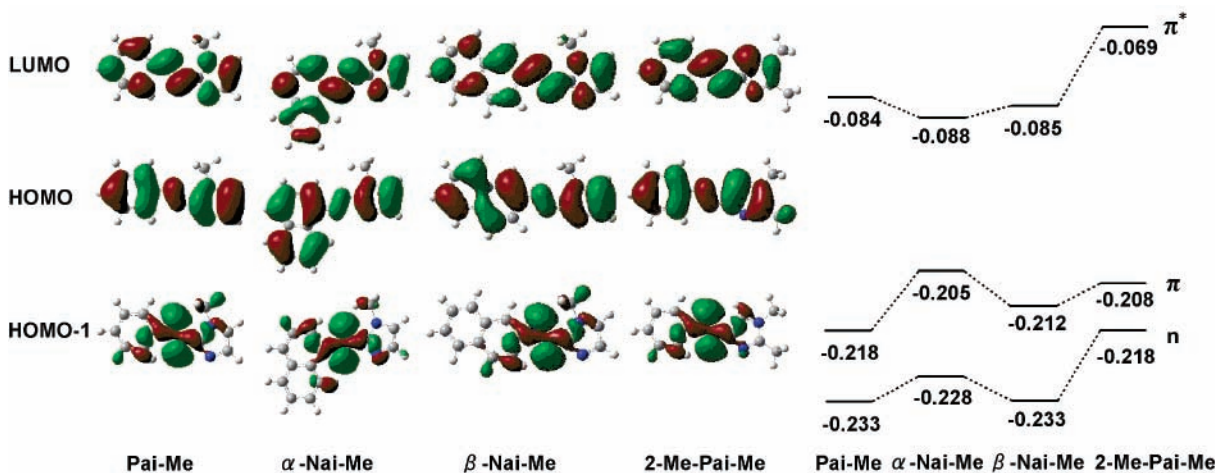


Figure 2. Frontier molecular orbitals of Pai-Me, α -Nai-Me, β -Nai-Me, and 2-Me-Pai-Me. Orbital energy values are given in hartrees in the diagram.

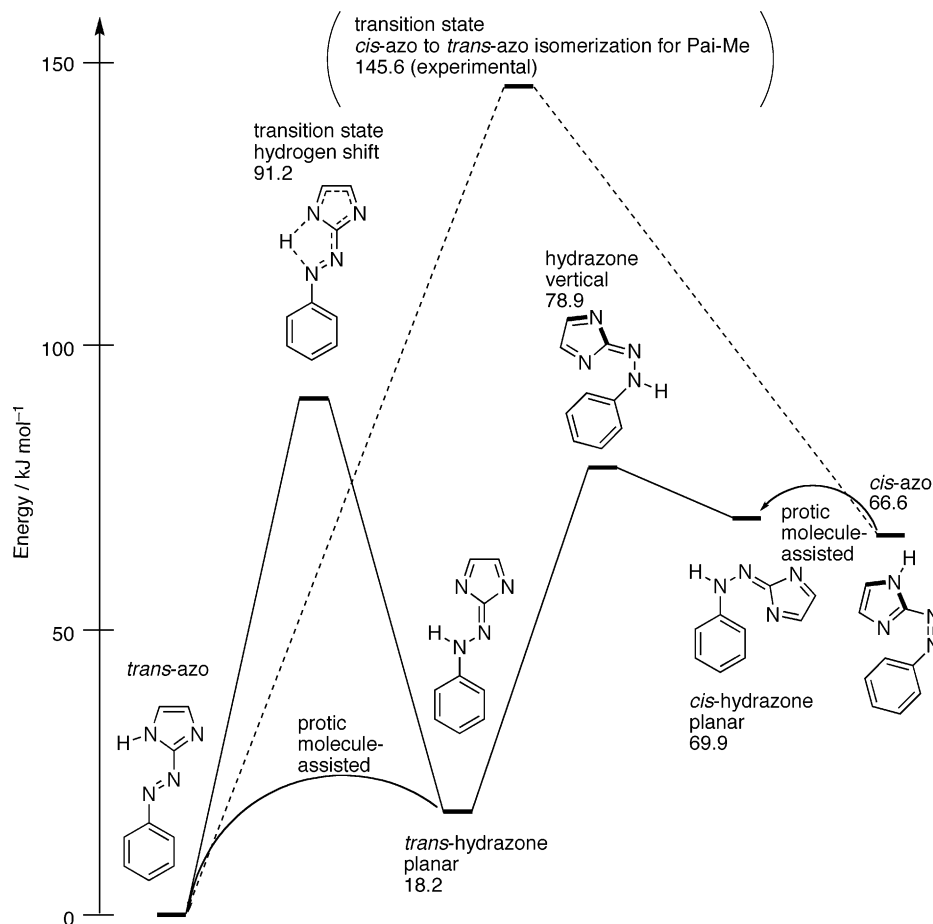


Figure 3. Energy diagram of representative stationary states for Pai-H according to DFT calculations. Values indicate energies relative to *trans*-azo in kJ mol^{-1} . The transition-state energy for the *cis*-azo to *trans*-azo reaction pathway ($145.6 \text{ kJ mol}^{-1}$) taken from experiments for Pai-Me (see ref 15) is included for comparison.

intermediate, the activation energy for the *cis*-to-*trans* isomerization of Pai-H could be much lower than that of Pai-Me. A direct reaction coordinate connecting the *cis*-azo form and the *cis*-hydrazone form, however, was not found. Either in the *trans* or in the *cis* configuration, an intramolecular hydrogen bond is improbable that could provide a reaction path for hydrogen transfer and consequent tautomerization. In this respect, this system is different from some azobenzene³⁶ and stilbene derivatives,^{37–39} in which an intramolecular hydrogen bond affects the course of the isomerization reaction through hydrogen transfer processes or preferential stabilization of a certain configuration.

Because it turned out that a direct intramolecular hydrogen shift reaction from the *cis*-Pai-H is unlikely, we then examined the effects of concentration and solvents on the rate of thermal *cis*-to-*trans* isomerization rate, experimentally. The idea behind the experiments is that if the thermal *cis*-to-*trans* isomerization is facilitated via tautomerization, protic substances may well accelerate the reaction via *intermolecular* hydrogen bonding. Pai-H itself could work as a proton donor through self-association.³⁴ In this case, the thermal isomerization should be accelerated as the Pai-H concentration is increased. The effects of other protic and nonprotic polar solvents were also investigated.

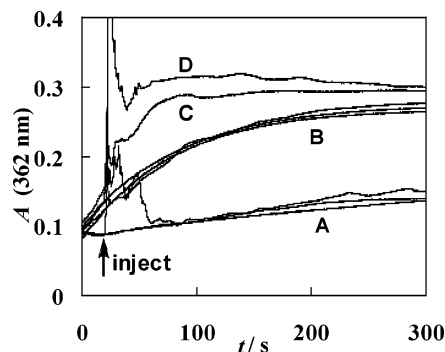


Figure 4. Effects of additives on the thermal cis-to-trans isomerization rate of Pai-H and Pai-Me. Traces in group A are for Pai-Me in toluene, toluene + 1% methanol, and toluene + 1% acetonitrile. Traces in group B are for Pai-H in toluene (as received and distilled from Na), toluene + 1% acetonitrile. Trace C is for Pai-H in toluene + 0.1% methanol. Trace D is for Pai-H in toluene + 1% methanol.

The thermal isomerization reaction was followed for Pai-Me and Pai-H in a concentration range between 4 and 130 μM in toluene. No concentration dependence was observed for Pai-Me; the isomerization rate for Pai-Me is characterized by the same $k_{c \rightarrow t}$ value. In contrast, the thermal isomerization rate for Pai-H was found to be concentration dependent. The rate was in proportion to the 0.43rd power of the total concentration of Pai-H and was fitted by an empirical equation: $v = k'_{c \rightarrow t} [\text{cis-Pai-H}] ([\text{cis-Pai-H}] + [\text{trans-Pai-H}])^{0.43}$ with $k'_{c \rightarrow t} = 1.9 \text{ M}^{-0.43} \text{ s}^{-1}$ in the studied concentration range. Thus, it is proved that the isomerization reaction is self-catalyzed through intermolecular interactions, most likely through intermolecular hydrogen bonding.

Figure 4 shows the time course of the absorbance at the λ_{max} of the $\pi\pi^*$ transition in pristine toluene and in toluene with small amounts of additional solvents during the cis-to-trans isomerization. In toluene, the cis-to-trans reaction of Pai-H takes place according to a trace in group B. In another run, 30 μL of methanol was added at $t = 20 \text{ s}$ (trace D) to a 3 mL toluene solution. After some initial turbulence due to mixing, the cis-to-trans conversion had been completed when the mixed solution was settled, which was within 30 s. Even as little as 3 μL of methanol enhanced the rate significantly as indicated by trace C. On the other hand, acetonitrile had no effect on the time course, the trace for which is within group B. In the same set of experiments for Pai-Me, the addition of neither methanol nor acetonitrile affected the time course of the cis-to-trans thermal reaction; all traces are within group A. From these results, it can be concluded that a protic molecule greatly enhances the cis-to-trans conversion only in the case of Pai-H, which has a dissociable imidazole hydrogen.

These data, taken together, support the view that the rapid thermal cis-to-trans isomerization for arylazoimidazoles without a substituent on the imidazole nitrogen occurs via the hydrazone tautomers, the formation of which is self-catalyzed and is promoted by protic molecules.

Conclusions

We have examined photoisomerization and thermal isomerization of an extensive series of arylazoimidazoles. Main findings follow: (1) The quantum yields of trans-to-cis photoisomerization are generally larger than those of azobenzene. (2) The quantum yields differ depending on the irradiation wavelength, as observed for azobenzene derivatives. (3) Thermal cis-to-trans isomerization is faster than that of azobenzene and is comparable to those of 4-*N,N*-dimethylaminoazobenzene and

4-nitroazobenzene. (4) Especially noteworthy feature is a very fast thermal cis-to-trans isomerization of arylazoimidazoles with no substituent on the imidazole nitrogen. This is especially so in the presence of protic solvents. The self-catalyzed and protic molecule-assisted tautomerization is proposed as the reason for the facile isomerization.

It is anticipated that the interplay of photochromic reaction and metal ion coordination leads to new functional materials. Studies on the effects of coordination to metal ions on the photochromic reactivity and, conversely, photomodulation of the properties of coordination complexes are underway in our laboratories.

Acknowledgment. This work was partially supported by the "High-Tech Research Center" Project for Private Universities: matching fund subsidy from the Ministry of Education, Culture, Sports, Science and Technology, Japan. C.S. thanks the Council of Scientific and Industrial Research, New Delhi, India, for financial support.

Supporting Information Available: Representative data for determining the absorption (Figure S1) and NMR (Figure S2) spectra of pure cis isomers and a table of the optimized coordinates by the DFT calculations. This material is available free of charge via the Internet at <http://pubs.acs.org>.

References and Notes

- Rau, H. In *Photochromism, Molecules and Systems*; Dürr, H., Bounas-Laurent, H., Eds.; Elsevier: Amsterdam, 1990; pp 165–192.
- Nishihara, H. *Bull. Chem. Soc. Jpn.* **2004**, *77*, 407–428.
- Tamai, N.; Miyasaka, H. *Chem. Rev.* **2000**, *100*, 1857–1890.
- Yagai, S.; Karatsu, T.; Kitamura, A. *Chem. Eur. J.* **2005**, *11*, 4054–4063.
- Chand, B.; Ray, U.; Mostafa, G.; Lu, T.-H.; Sinha, C. *J. Coord. Chem.* **2004**, *57*, 627–634.
- Ray, U.; Banerjee, D.; Mostafa, G.; Lu, T.-H.; Sinha, C. *New J. Chem.* **2004**, *28*, 1437–1442.
- Dinda, J.; Jasimuddin, S.; Mostafa, G.; Hung, C.-H.; Sinha, C. *Polyhedron* **2004**, *23*, 793–800.
- Jasimuddin, S.; Sinha, C. *Transition Met. Chem.* **2004**, *29*, 566–570.
- Chand, B. G.; Ray, U. S.; Mostafa, G.; Cheng, J.; Lu, T.-H.; Sinha, C. *Inorg. Chim. Acta* **2005**, *358*, 1927–1933.
- Raj, S. S. S.; Fun, H.-K.; Chen, X.-F.; Zhu, X.-H.; You, X.-Z. *Acta Crystallogr.* **1999**, *C55*, 1644–1646.
- Dash, A. C.; Acharya, A.; Sahoo, R. K. *Indian J. Chem.* **1998**, *37A*, 759–764.
- Ackermann, M. N.; Robinson, M. P.; Maher, I. A.; LeBlanc, E. B.; Raz, R. V. *J. Organomet. Chem.* **2003**, *682*, 248–254.
- Endo, M.; Nakayama, K.; Kaida, Y.; Majima, T. *Tetrahedron Lett.* **2003**, *44*, 6903–6906.
- Fukuda, N.; Kim, J. Y.; Fukuda, T.; Ushijima, H.; Tamada, K. *Jpn. J. Appl. Phys.* **2006**, *45*, 460–464.
- Otsuki, J.; Suwa, K.; Narutaki, K.; Sinha, C.; Yoshikawa, I.; Araki, K. *J. Phys. Chem. A* **2005**, *109*, 8064–8069.
- For Pai-H, Pai-Me, Pai-Et, and Cai-Me, see: Misra, T. K.; Das, D.; Sinha, C. *Polyhedron* **1997**, *16*, 4163–4170.
- For Pai-Bn and Tai-Bn, see: Ray, U. S.; Mostafa, G.; Lu, T. H.; Sinha, C. *Cryst. Eng.* **2002**, *5*, 95–104.
- For Tai-H, Tai-Me, and Tai-Et, see: Bag, K.; Misra, T. K.; Sinha, C. *J. Indian Chem. Soc.* **1998**, *75*, 421–422.
- For 4-Me-Pai-H and 2-Me-Pai-H, see: Fargher, R. G.; Pyman, F. L. *J. Chem. Soc. Trans.* **1919**, *115*, 217–260.
- For α -Nai-H, α -Nai-Me, α -Nai-Et, and α -Nai-Bn, see: Byabartta, P.; Santra, P. K.; Misra, T. K.; Sinha, C.; Kennard, C. H. L. *Polyhedron* **2001**, *20*, 905–913.
- For β -Nai-H, β -Nai-Me, β -Nai-Et, and β -Nai-Bn, see: Pal, S.; Das, D.; Chattopadhyay, P.; Sinha, C.; Panneerselvam, K.; Lu, T. H. *Polyhedron* **2000**, *19*, 1263–1270.
- For 2-Me-Pai-Me, see: Maciejewska, D. *Pol. J. Chem.* **1995**, *69*, 1638–1641.
- Zimmerman, G.; Chow, L.; Paik, U. *J. Am. Chem. Soc.* **1958**, *80*, 3528–3531.
- Frisch, M. J.; Trucks, G. W.; Schlegel, H. B.; Scuseria, G. E.; Robb, M. A.; Cheeseman, J. R.; Montgomery, J. A., Jr.; Vreven, T.; Kudin, K.

- N.; Burant, J. C.; Millam, J. M.; Iyengar, S. S.; Tomasi, J.; Barone, V.; Mennucci, B.; Cossi, M.; Scalmani, G.; Rega, N.; Petersson, G. A.; Nakatsuji, H.; Hada, M.; Ehara, M.; Toyota, K.; Fukuda, R.; Hasegawa, J.; Ishida, M.; Nakajima, T.; Honda, Y.; Kitao, O.; Nakai, H.; Klene, M.; Li, X.; Knox, J. E.; Hratchian, H. P.; Cross, J. B.; Bakken, V.; Adamo, C.; Jaramillo, J.; Gomperts, R.; Stratmann, R. E.; Yazyev, O.; Austin, A. J.; Cammi, R.; Pomelli, C.; Ochterski, J. W.; Ayala, P. Y.; Morokuma, K.; Voth, G. A.; Salvador, P.; Dannenberg, J. J.; Zakrzewski, V. G.; Dapprich, S.; Daniels, A. D.; Strain, M. C.; Farkas, O.; Malick, D. K.; Rabuck, A. D.; Raghavachari, K.; Foresman, J. B.; Ortiz, J. V.; Cui, Q.; Baboul, A. G.; Clifford, S.; Cioslowski, J.; Stefanov, B. B.; Liu, G.; Liashenko, A.; Piskorz, P.; Komaromi, I.; Martin, R. L.; Fox, D. J.; Keith, T.; Al-Laham, M. A.; Peng, C. Y.; Nanayakkara, A.; Challacombe, M.; Gill, P. M. W.; Johnson, B.; Chen, W.; Wong, M. W.; Gonzalez, C.; Pople, J. A. *Gaussian 03*, revision C.02; Gaussian, Inc.: Wallingford, CT, 2004.
- (25) Beck, A. D. *J. Chem. Phys.* **1993**, *98*, 5648–5652.
- (26) Dunning, T. H., Jr. *J. Chem. Phys.* **1989**, *90*, 1007–1023.
- (27) Nishimura, N.; Sueyoshi, T.; Yamanaka, H.; Imai, E.; Yamamoto, S.; Hasegawa, S. *Bull. Chem. Soc. Jpn.* **1976**, *49*, 1381–1387.
- (28) Brown, E. V.; Granneman, G. R. *J. Am. Chem. Soc.* **1975**, *97*, 621–627.
- (29) Yoshida, K.; Koujiri, T.; Horii, T.; Kubo, Y. *Bull. Chem. Soc. Jpn.* **1990**, *63*, 1658–1664.
- (30) Bhunia, P.; Baruri, B.; Ray, U.; Sinha, C.; Das, S.; Cheng, J.; Lu, T.-H. *Transition Met. Chem.* **2006**, *31*, 310–315.
- (31) Fun, H.-K.; Chinnakali, K.; Chen, X.-F.; Zhu, X.-H.; You, X.-Z. *Acta Crystallogr.* **1999**, *C55*, IUC9900025.
- (32) Maciejewski, D.; Skulski, L. *Pol. J. Chem.* **1981**, *55*, 2105–2121.
- (33) Maciejewska, D.; Skulski, L. *Pol. J. Chem.* **1983**, *57*, 971–984.
- (34) Gabor, G.; Frei, Y. F.; Fischer, E. *J. Phys. Chem.* **1968**, *72*, 3266–3272.
- (35) Fischer, E.; Frei, Y. F. *J. Chem. Soc.* **1959**, 3159–3163.
- (36) Gabor, G.; Fischer, E. *J. Phys. Chem.* **1962**, *66*, 2478–2481.
- (37) Arai, T.; Iwasaki, T.; Tokumaru, K. *Chem. Lett.* **1993**, 691–694.
- (38) Lewis, F. D.; Yoon, B. A.; Arai, T.; Iwasaki, T.; Tokumaru, K. *J. Am. Chem. Soc.* **1995**, *117*, 3029–3036.
- (39) Norikane, Y.; Itoh, H.; Arai, T. *J. Phys. Chem. A* **2002**, *106*, 2766–2776.